11th World Congress on Structural and Multidisciplinary Optimisation
07th -12th, June 2015, Sydney Australia

Optimal design of a double coil magnetorheological fluid damper with various piston profiles

Guoliang Hu[1, 2], Zheng Xie[1], Weihua Li[2, *]

[1]School of Mechatronic Engineering, East China Jiaotong University, Nanchang City, Jiangxi Province, China, glhu@ecjtu.edu.cn
[2]School of Mechanical, Materials and Mechatronic Engineering, University of Wollongong, NSW, Australia, weihuali@uow.edu.au

Abstract
A magnetorheological (MR) damper is one of the most advanced devices used in a semi-active control system to mitigate unwanted vibration because the damping force can be controlled by changing the viscosity of the internal magnetorheological fluids (MRF). This study proposes a typical double coil MR damper where the damping force and dynamic range were derived from a quasi-static model based on the Bingham model of MR fluid. A finite element model was built to study the performance of this double coil MR damper by investigating seven different piston configurations, including the numbers and shapes of their chamfered ends. The objective function of an optimisation problem was proposed and then an optimisation procedure was constructed using the ANSYS parametric design language (APDL) to obtain the optimal value of a double coil MR damper. Furthermore, an experimental analysis was also carried out. These results were then compared with the optimised MR damper's simulation results, which clearly validated the simulated results. The relevant results of this analysis can easily be extended to other MR dampers.
Keywords: MRF, MR damper, Double coil, Finite element analysis, Optimal design

1. Introduction

The rheological properties of a magnetorheological fluid (MRF) can be continuously changed within several milliseconds by applying or removing external magnetic fields. These unique features have led to the development of many MRF-based devices such as the MR damper, MR valve, MR brake, MR clutch, and so on.

Recently, some studies in literature have focused on the geometric optimisation of an MR damper, with the results showing that their performance can be improved significantly by optimising the design of the magnetic circuit that controls these systems. Zhang et al. [1] proposed the use of finite elements to improve the magnetic design of an MR damper. Kham et al. [2] used finite element software to simulate nine different configurations of the pistons for an MR damper and investigate how these configurations would affect and influence the maximum pressure drop; the results showed that a single coil piston with chamfered ends was better than the other configurations for the same magnitude of input current and piston velocity. Ferdaus et al. [3] established 2D axi-symmetric and a 3D model of an MR damper that considered the shape of the piston, the MR fluid gap, the air gap, and the thickness of the damper's housing. All these models were simulated with different currents, different piston velocities, and different strokes. Parlak et al. [4] investigated the geometrical optimisation of an MR shock damper using the Taguchi experimental design approach by specifying four parameters (gap, flange thickness, radius of piston core, and current excitation) and by selecting the maximum dynamic range required as the target value; this analysis was carried out using analytical equations rather than experimental data. Parlak et al. [5] presented a method for optimising the design of the target damper force and maximum magnetic flux density of an MR damper; this new approach used an electromagnetic analysis of the magnetic field and a CFD analysis of MR flow together to obtain the optimal value of the design parameters. Nguyen and Choi [6] presented an optimal design of a passenger vehicle MR damper that was constrained in a specific cylindrical volume, and an advanced objective function that collectively included the damping force, the dynamic range, and an inductive time constant. Nguyen and Choi [7] also proposed two types of shear mode MR dampers for a front loader washing machine, where an optimisation methodology based on a finite element analysis integrated with an optimisation tool was used to obtain the optimal geometric dimensions of the MR dampers; the results showed that an MR damper with three coils and without a non-magnetic bobbin was the best configuration for this application.

In this study a double coil MR damper was developed and prototyped, and the damping force and dynamic range were also derived. A finite element model was built to investigate the performance of the double coil MR damper by considering seven pistons with different configurations. An optimisation procedure was then constructed with the ANSYS parametric design language (APDL) to obtain the optimal parameters of the double coil MR damper. Finally, a series of dynamic experimental tests were also carried out.

2. Design considerations for a double coil MR damper with an annular gap

Figure 1 shows a schematic for the proposed double coil MR damper under consideration. Two chambers in the cylinder are separated by a floating piston. The section with the piston head is filled with MR fluid and the accumulator that compensates for the changes in volume induced as the piston rod moves is filled with pressurised nitrogen gas. As the damper piston rod moves, the MR fluid flows through the annular gap to the other side of the piston. There is a double coil of wire inside the piston head used for winding is heat resistant and electrically insulated. When a direct current is applied to the double coil, a magnetic field occurs around the piston head. It is noted that the direction of the current applied onto the double coil can be the same or the reverse, and it can enlarge the maximum damping force or the dynamic range to some extent.

Figure 2 shows the magnetic circuit of the double coil MR damper with an annular gap at both ends of the flanges and in the middle of the flange, where the flux lines are perpendicular to the flow direction and caused a field-dependent resistance to the fluid flow. The double coil MR damper is shaped to guide the magnetic flux axially through the damper core, across the length of the core flange and the gap at one end, then on through the flux return and across the gap and core flange at the opposite end. The volume of fluid through which the magnetic field passes is defined as an active volume, and the MR effects only occur within the active volume. The most effective MR dampers have a high magnetic flux density passing through a large active volume, but a lot of magnetic coils are needed to produce large magnetic fields. An optimised circuit would maintain a balance between the field produced and power required by the magnetic coils.

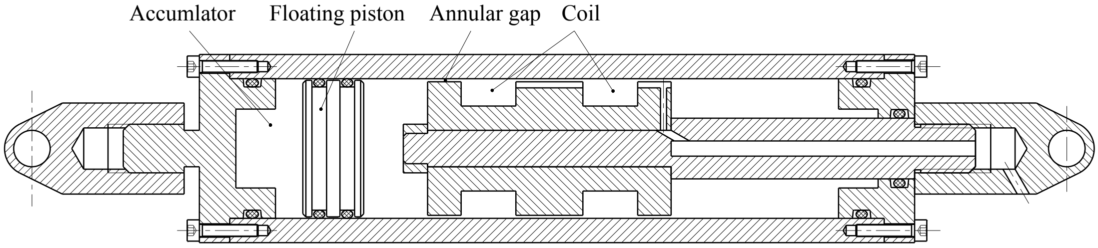

Figure 1: Schematic diagram of a double coil MR damper with annular gap

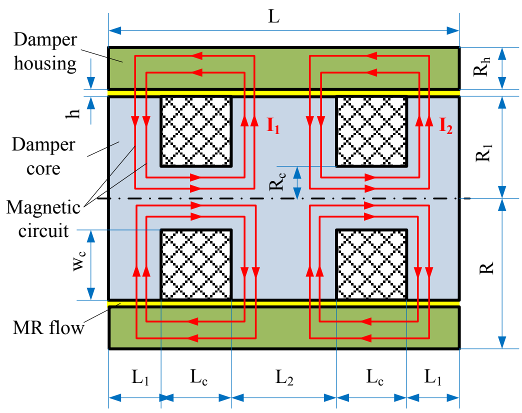

Figure 2: Magnetic circuit of the double coil MR damper with annular gap

Some of the important dimensions of double coil MR damper are also listed in Fig.2. Damper geometry is characterised by the length of the gap L, the length of the end flange L_1, the length of the middle flange L_2, the length of the coil L_c, the thickness of the piston head housing R_h, the width of the annular gap h, the radius of the piston head R, the internal radius of the piston core R_c, the external radius of the piston core R_1, and the width of the coil W_c.

The total damping force F generated by the double coil MR damper consists of three components: the field-dependent force F_τ due to the magnetic field, the viscous force F_η due to the viscous effects, and the frictional force F_f.

$$F = F_\tau + F_\eta + F_f \tag{1}$$

where

$$F_\eta = \frac{6\eta L q A_p}{\pi(R_1 + 0.5h)h^3} \tag{2}$$

$$F_\tau = 2c_1 \frac{L_1}{h} A_p \tau_{y1} \operatorname{sgn}(v_p) + c_2 \frac{L_2}{h} A_p \tau_{y2} \operatorname{sgn}(v_p) \tag{3}$$

where A_p is the cross-sectional area of the piston head, and η is the plastic viscosity. q is the flow rate through the double coil MR damper, and it can be calculated from the velocity of the piston v_p. τ_{y1} and τ_{y2} are the yield stresses of the MR fluid in the end flange and middle flange, respectively. c_1 and c_2 are coefficients which depended on the flow velocity profile, and have a value ranging from a minimum value of 2.07 to a maximum value of 3.07.

As shown in Eq. (1), the first term is called the controllable force because it varies with the applied field, whereas the sum of the latter two terms is referred to as the uncontrollable force because they generate a constant force according to the velocity of the piston.

The dynamic range D is defined as the ratio of the total damping force to the uncontrollable force, and it is given by

$$D = \frac{F_\tau + F_\eta + F_f}{F_\eta + F_f} = 1 + \frac{F_\tau}{F_\eta + F_f} \tag{6}$$

Here, the dynamic range D was introduced to evaluate the performance of the double coil MR damper. Normally, it is better to keep the dynamic range as large as possible to maximise the effectiveness of the MR damper. The dynamic range is proportional to the shear force and is a function of the size of the gap. The width of the annular gap h is inversely proportional to the controllable force, so a small gap width will increase the range of the controllable force, but when h is less than 0.5 mm, the viscous force F_η is much faster than the controllable force F_τ' this reduces the dynamic range. Again when the gap becomes wider both F_τ and F_η fall, so finding an optimal width gap that maximises the dynamic range is very important. Moreover, parameters such as the length of the flange L_1 and L_2, the radius of the piston head R, the yield stress τ_{y1} and τ_{y2}, the thickness of the piston head housing R_h and the internal radius of the core of the piston R_c will also play an important role in searching for the right design.

3. Modelling an optimal design of a double coil MR damper using the finite element method

The magnetic field in an MR damper is produced by an electromagnet. Here in the ANSYS simulation model the excitation coil is considered to be the electromagnet, and the magnetic field provided by this excitation coil is needed to energise the MR fluid. By varying the current through the excitation coil the density of the magnetic flux can be varied and the MR fluid is energised accordingly.

To investigate how the shape of the piston affects the performance of a double coil MR damper, seven models with different shaped pistons were designed, as shown in Fig.3. The model 1 piston was defined as having a plain end, the model 2 piston was defined as have each end of the piston chamfered, the model 3 piston was defined as having a radius on each end, the model 4 piston was defined as having chamfers on the top, bottom, and in the middle, the model 5 piston was defined as having a radius on the top, bottom and in the middle, the model 6 piston was defined as having both ends chamfered, and the model 7 piston was defined as having a radius on every edge.

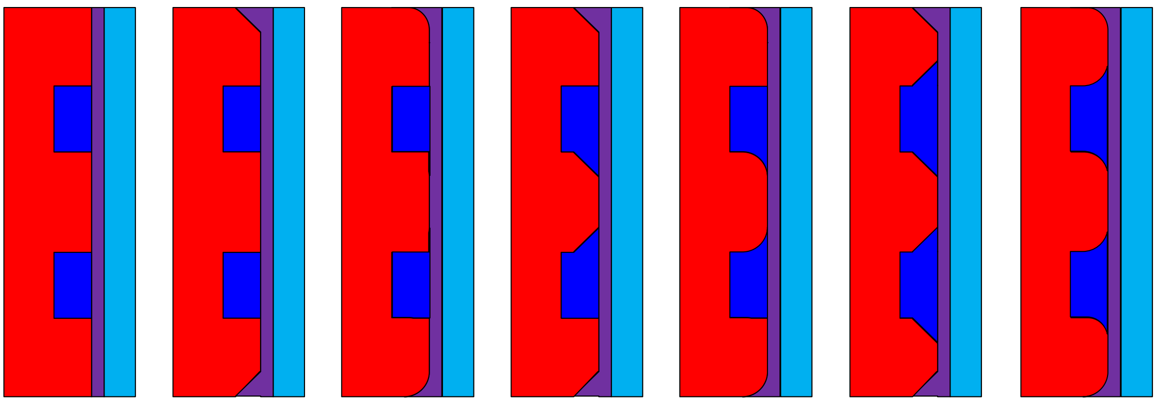

(a) Model 1 (b) Model 2 (c) Model 3 (d) Model 4 (e) Model 5 (f) Model 6 (g) Model 7

Figure 3: Simulation models with different piston shapes

Figure 4 shows the results of the magnetic flux densities between the different models when the current varied from 0.1A to 1.0A. Here the magnetic flux densities decreased with the number of chamfers on the damper piston, the maximum density of magnetic flux appeared in Model 1, which means that this piston had the optimal geometrical shape. Moreover, density of magnetic flux in the model with a radius was greater than the chamfered model; the reason can be found in Figure 5 which shows that the distribution of magnetic flux lines along the resistance gap in model 1 were more even that in models 6 and 7. The damper piston with chamfers had larger reluctances at its core because is the core was larger and the cross-sectional area through which the magnetic flux passed decreased, which in turn caused the magnetic flux densities in the fluid resistance gap to decrease as well.

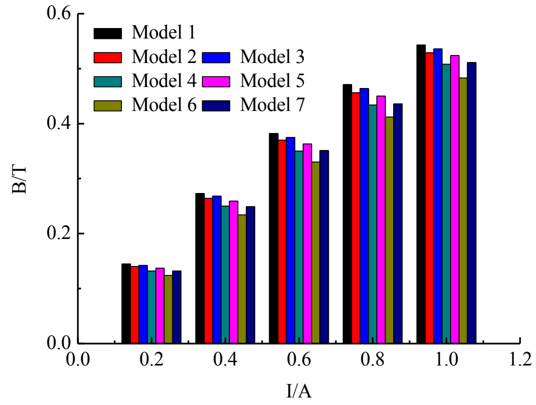

Figure 4: Magnetic flux density of different models

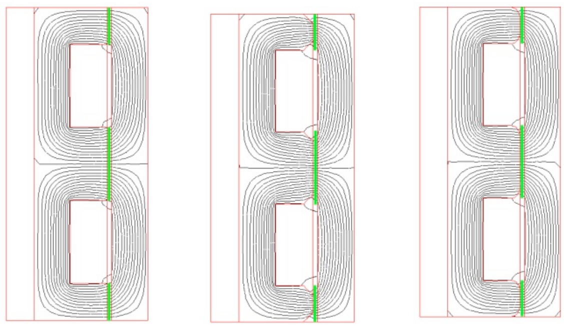

(a) Model 1 (b) Model 6 (c) Model 7

Figure 5: Distributions of magnetic flux lines of different models

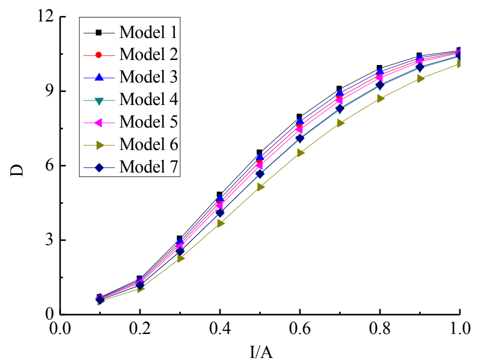

Figure 6: Dynamic range of MR damper under different currents

Figure 6 shows the dynamic range of the proposed MR damper under different piston configurations when the applied current varied from 0.1A to 1.0A. Here the dynamic range decreased as the number of chamfers on the pistons increased, and so too did the damping performance. Moreover, the dynamic range in the model with a radius on the edges was greater than the model with chamfered edges. When the current varied from 0.1A to 1.0A, the damping force steadily increased and then stabilised when the current was close to 1.0A due to the magnetic saturation of MRF in the resistance gap. From Figure 4 to Figure 6, model 1 with square ends had the maximum B value under different currents, while the damping force and dynamic range was also better in model 1 than in the other models. So the piston with square ends was selected as the optimal geometry for the double coil MR damper.

To optimise the double coil MR damper using FEM, an analysis log file to solve the damper's magnetic circuit calculate the objective function was built using the ANSYS parametric design language (APDL). In the analytical log file, the length of resistance L_1 and the radius of the damper core r_1 were used as the design variables (DVs), and initial values were assigned to them, respectively. First, starting with the initial values of the DVs, the magnetic flux density, damping force and dynamic range were calculated by executing the log file. The ANSYS optimisation tool then transformed the optimisation problem with constrained DVs to an unconstrained one via penalty functions. The search direction of DVs was assumed to be the negative of the gradient of unconstrained objective function, and a combination of a golden-section algorithm and local quadratic fitting techniques were used to calculate new DVs. If convergence occurs, the DVs at this iteration would be the optimum, but if not then subsequent iterations would be carried out.

Figure 7 shows the results of the damping force between the initial design and optimal design, respectively. Here the damping force with an optimal design was greater than the initial design, although the difference between both of them improved significantly when the applied current exceeded 0.5A.

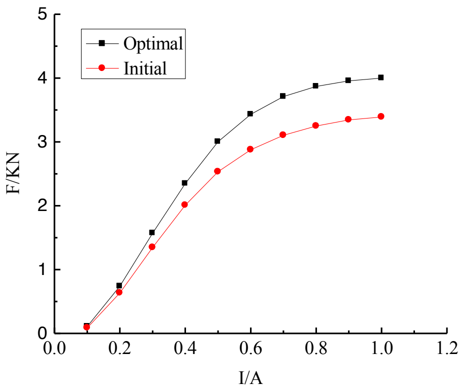

Figure 7: Comparison of damping force between initial design and optimal design

4. Experimental evaluation of double coil MR damper

Figure 8 shows the change in the damping force under different damper displacements and applied current directions. Here, the INSTRON 8801 test machine was set at sinusoidal loading with a frequency of 0.5Hz and displacement amplitude of 5mm and 7.5mm, respectively. The applied current I_1 and I_2 in the double coils were set to 0.5A with the same direction and reverse direction, respectively. The figure shows that the damping force with the currents in a reverse direction were much greater that currents in the same direction. Moreover, the damping force increased as the displacement amplitude increased, because the increased velocity of the damper led to an increase in the viscous force in Eq.(2), so the damping force also increased.

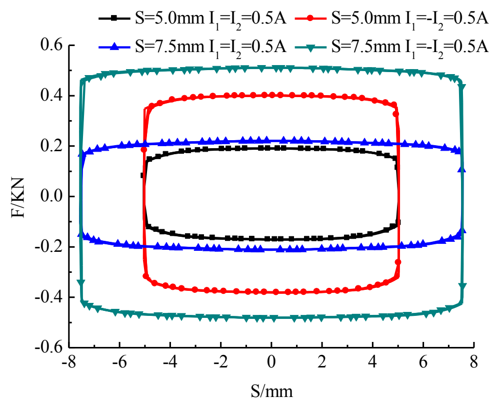

Figure 8: Damping forces under different displacements and different current directions

Figure 9 shows the damping force under the applied currents changed from 0A to 1.0A. Here, the INSTRON 8801 test machine was set at a sinusoidal loading with displacement amplitude of 10mm and a frequency of 1.0Hz, while the applied currents I_1 and I_2 in the double coils were applied the reverse direction. As expected, the damping force increased from 0.33KN at 0A to 1.21KN at 1.0A, and the dynamic range nearly equal 4.

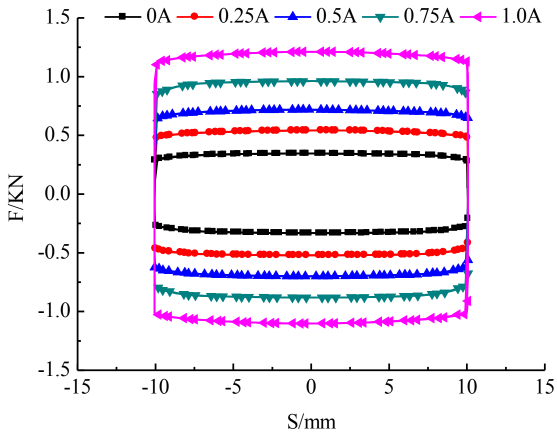

Figure 9: Damping force under different current

5. Conclusion

A double coil MR damper was proposed and the damping force and dynamic range were also derived. A finite element model was built to investigate the performance of a double coil MR damper while considering pistons with different configurations; the simulation results showed that the piston with square ends had a better damping performance. An optimisation procedure was constructed using the ANSYS APDL to obtain the optimal value of the double coil MR damper. Further, an experimental analysis was also carried out to verify the damping performance of the proposed MR damper.

6. Acknowledgements

This research was financially supported by the National Natural Science Foundation of China (No. 51475165, 51165005, 11462004) and the Australian Research Council Discovery Project (No. 1501002636).

7. References

[1] H. H. Zhang, C. R. Liao and W. M. Chen, A magnetic design method of MR fluid dampers and FEM analysis on magnetic saturation, *Journal of intelligent material systems and structures*, 17(8-9), 813-818, 2006.

[2] M. S. A. Khan, A. Suresh, N. S. Ramaiah, Analysis of magnetorheological fluid damper with various piston profiles. *International Journal of Engineering and Advanced Technology*, 2(2), 77-83, 2012.

[3] M. M. Ferdaus, M. M. Rashid and M. H. Hasan, Optimal design of Magneto-Rheological damper comparing different configurations by finite element analysis, *Journal of mechanical science and technology*, 28(9), 3667-3677, 2014.

[4] Z. Parlak, T. Engin and V. Ari. Geometrical optimisation of vehicle shock dampers with magnetorheological fluid, *International journal of vehicle design*, 54(4), 371-392, 2010.

[5] Z. Parlak, T. Engin and İ Çallı, Optimal design of MR damper via finite element analyses of fluid dynamic and magnetic field, *Mechatronics*, 22(6), 890-903, 2012.

[6] Q. H. Nguyen and S. B. Choi, Optimal design of a vehicle magnetorheological damper considering the damping force and dynamic range, *Smart Materials and Structures*, 18(1), 015013, 2009.

[7] Q. H. Nguyen, S. B. Choi and J. K. Woo, Optimal design of magnetorheological fluid-based dampers for front-loaded washing machines, *Proceedings of the Institution of Mechanical Engineers, Part C: Journal of Mechanical Engineering Science*, 228(2), 294-306, 2014.